Accepted Manuscript

Taniaphos·AgF-catalyzed enantioselective 1,3-dipolar cycloaddition of stabilized azomethine ylides derived from 2,2-dimethoxyacetaldehyde

Alberto Cayuelas, Olatz Larrañaga, Carmen Nájera, José M. Sansano, Abel de Cózar, Fernando P. Cossío

PII: S0040-4020(16)30640-8

DOI: 10.1016/j.tet.2016.07.017

Reference: TET 27913

To appear in: *Tetrahedron*

Received Date: 8 February 2016

Revised Date: 20 June 2016

Accepted Date: 5 July 2016

Please cite this article as: Cayuelas A, Larrañaga O, Nájera C, Sansano JM, de Cózar A, Cossío FP, Taniaphos·AgF-catalyzed enantioselective 1,3-dipolar cycloaddition of stabilized azomethine ylides derived from 2,2-dimethoxyacetaldehyde, *Tetrahedron* (2016), doi: 10.1016/j.tet.2016.07.017.

Graphical Abstract

To create your abstract, type over the instructions in the template box below.
Fonts or abstract dimensions should not be changed or altered.

Taniaphos·AgF-catalyzed enantioselective 1,3-dipolar cycloaddition of stabilized azomethine ylides derived from 2,2-dimethoxyacetaldehyde

A. Cayuelas , O. Larrañaga, C. Nájera, J. M. Sansano,* A. de Cózar,* F. P. Cossío

Leave this area blank for abstract info.

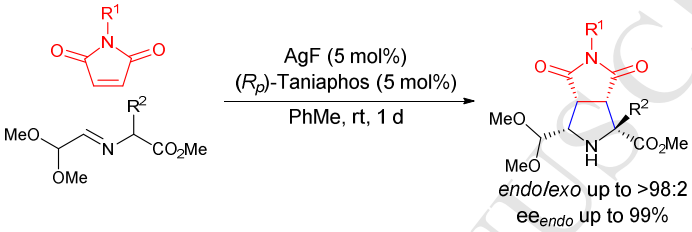

Tetrahedron
journal homepage: www.elsevier.com

Taniaphos·AgF-catalyzed enantioselective 1,3-dipolar cycloaddition of stabilized azomethine ylides derived from 2,2-dimethoxyacetaldehyde

Alberto Cayuelas,[a,b,c] Olatz Larrañaga,[c,d] Carmen Nájera,[a,c] José M. Sansano,[a,b,c]* Abel de Cózar,[c,d,e]* Fernando P. Cossío[c,d]

[a] Departamento de Química Orgánica, Universidad de Alicante, Apdo. 99, E-03080-Alicante, Spain.
[b] Instituto de Síntesis Orgánica (ISO), Universidad de Alicante, Spain.
Fax: (+34)-965-903-549; phone: (+34)-965-903-549; Corresponding author; e-mail: jmsansano@ua.es
[c] Centro de Innovación en Química Avanzada (ORFEO-CINQA), Spain
[d] Departamento de Química Orgánica I, Facultad de Química, Universidad del País Vasco, P. K. 1072, E-20018 San Sebastián, Spain.
[e] IKERBASQUE, Basque Foundation for Science, 48011 Bilbao, Spain. Corresponding author for theoretical studies. abel.decozar@ehu.es,

Abstract: The enantioselective Taniaphos·silver fluoride-catalyzed enantioselective 1,3-dipolar cycloaddition using 2,2-dimethoxyacetaldehyde derived imino esters and maleimides is described. The employment of this complex allows the reaction in the absence of an extra base giving high yields and *ee* of the corresponding *endo*-cycloadducts. Calculations performed at B3LYP/6-31G*&LANL2DZ level of theory predicted the expected absolute stereochemistry for both BINAP and Taniaphos·silver fluoride-mediated cycloadditions, as well as the enantioselectiviy and mild conditions of the reaction.

Keywords: dipolar cycloaddition · taniaphos · silver(I) · enantioselective · 2,2-dimethoxyacetaldehyde·azomethine ylides

Dedicated to Prof. Gary Posner on the occasion of his retirement

1. Introduction

1,3-Dipolar cycloadditions (1,3-DCs)[1] involving stabilized azomethine ylides are fascinating reactions[2] due to the high control of the regio-, diastereo- and enantioselection. However, they have limitations concerning the structure of the dipole precursor. Compared to arylideneamino esters, alkylideneamino esters are not found to be appropriate ylide precursors in conventional enantioselective metal-catalyzed 1,3-DC. In many cases In many cases, the corresponding imines are not formed quantitatively or even the stereoselectivity of the 1,3-DCs using different dipolarophiles is not very high. Regarding the asymmetric version of this 1,3-DC[3] many examples have been reported employing chiral Lewis acids (mainly metal complexes) and organocatalysts.

The resulting enantiomerically enriched prolines or pyrrolidines *endo*-**1** normally incorporate an aryl or heteroaryl substituent but rarely extend to cases that have an aliphatic group at the 5-position. Waters' group developed recently a 2-aza-Cope-[3+2] dipolar cycloaddition preparing α-allylproline derivatives with different substituents at the 5-position of the heterocyclic ring.[4] The interest of this objective is to gain a new functionalization on the pyrrolidine ring ready to be transformed into other different functionalities.

Following this idea, we recently reported the (*S*)-BINAP **4**·Ag_2CO_3-catalyzed enantioselective 1,3-DC using ethyl glyoxylate for the preparation of diastero- and enantiomerically enriched *endo*-pyrrolidines **2** with a 2,5-*cis*-arrangement. Because of the instability of the imino esters derived of ethyl glyoxylate this process was performed in a multicomponent fashion allowing the introduction of an ester group at the 5-position. In this case, use of a base was not necessary as the chiral complex behaved as a bifunctional catalyst.[5] The incorporation of a 2,2-dimethoxymethyl group at the 5-position (compound *endo*-**3**) was reported in a previous non asymmetric silver-catalyzed multicomponent reaction between 2,2-dimethoxyacetaldehyde, α-amino esters and dipolarohiles in the presence of triethylamine.[6]

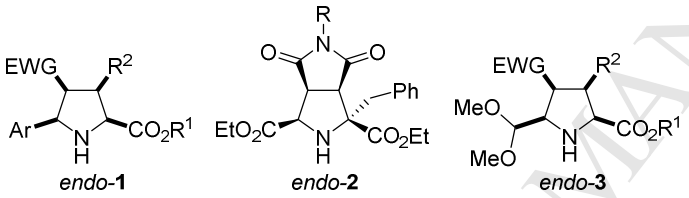

In this work we describe the introduction of the 2,2-dimethoxymethyl group at the 5-position of the final proline derivative employing the imino ester derived from 2,2-dimethoxyacetaldehyde and the corresponding amino ester, through an enantioselective process catalyzed by chiral silver complexes using chiral phosphorous ligands.[7]

2. Results and discussion

The synthesis of enantiomerically enriched prolinates *endo*-**3** was initially attempted using the best reaction conditions reported for the multicomponent synthesis of chiral *endo*-**2** cycloadducts,[5] using phenyl alanine ethyl ester, *N*-methylmaleimide (NMM, **5a**), 2,2-dimethoxyacetaldehyde and 5 mol% of the catalyst (*S*)-BINAP **4**·Ag_2CO_3. All these components were mixed and, after 1 d at room temperature, a very complex reaction crude was observed (^{1}H NMR). Unlike ethyl glyoxylate, 2,2-dimethoxyacetaldehyde was able to form, almost quantitatively, stable imino esters **6** which could be employed in a two-component cycloaddition. Thus, as a model reaction glycine derived imino ester **6a** and *N*-methylmaleimide (NMM, **5a**) were catalyzed by a complex formed by 5 mol% of a chiral ligand and 5 mol% of a silver(I) salt (Scheme 1). Initially, (*S*)-BINAP **4a**·AgTfa (Tfa = trifuoroacetate) as chiral catalyst was chosen.[8,9] In all of these cases, the chiral catalyst was formed in situ by mixing the corresponding chiral ligand with

the silver salt in toluene stirring the mixture for 30 min at room temperature (25 ºC). The evaluation of the importance of the organic base (5 mol%) in the reaction was done first. Cycloadduct **7aa** was obtained with high conversions and with 60% *ee* independently of the added base (triethylamine or DIPEA, Table 1, entries 1 and 2). However, a 64% *ee* was determined when the reaction was performed under identical conditions but in the absence of base (Table 1, entry 3). Looking for basic silver salts, carbonate, acetate, and benzoate were assayed (Table 1, entries 4-6). Silver carbonate was the most appropriate salt for the enantioselective multicomponent 1,3-DC involving ethyl glyoxylate,[5] nevertheless no improvement was observed in the enantiomeric excess of *endo*-**7aa** (Table 1, entry 4). AgOBz and AgOAc afforded *endo*-**7aa** with 65% and 60% *ee*, respectively (Table 1, entries 5 and 6). (*S*)-BINAP **4a**·AgF[10] was more efficient at room temperature rather than at -20 ºC, affording product *endo*-**7aa** with 72% *ee* (Table 1, entries 7 and 8).

The ligand was the next parameter to be changed. Thus, the small variation introduced with (*S*)-Tol-BINAP **4b** gave the same results as (*S*)-Binap (Table 1, entry 9). Modification of the bite angle using (*S*)-H8-BINAP **8** or (*S*)-Segphos **9** resulted in lower enantioselection in cycloadduct **7aa** (Table 1, entries 10 and 11). Widely used chiral phosphoramidites **10**-**14** were tested together with silver fluoride. Despite high conversions, the results of the corresponding enantioselectivities were very disappointing. (*S*)-Monophos **10** and (S_a,*R*,*R*)-phosphoramidites **11a** and **11b**[11,12] induced up to 26% *ee* (Table 1, entries 12-14) and almost racemic *endo*-**7aa** was obtained using phosphoramidite (*S*)-**13** (Table 1, entry 16). H8-Phosphoramidite **12** furnished comparable results to those obtained in the same reaction run with (*S*)-BINAP **4a**·AgTfa (Table 1, compare entries 3 and 15). Taddol derived phosphoramidite **14** afforded a crude *endo*-**7aa** product (60% *ee*) contaminated with some *endo/exo* diastereoisomers (Table 1, entry 17). Bisphosphanes **15**, **16** and **17** were allowed to form the corresponding chiral complex with AgF at room temperature and next evaluated in the model 1,3-DC shown in Scheme 1. (*R*,*R*)-Me-Duphos **15** gave lower conversion and a 6% *ee* of **7aa** (Table 1, entry 18). (*R*,S_p)-Josiphos **16** and (R_p)-Taniaphos **17** furnished the opposite enantiomer *ent*-*endo*-**7aa** in excellent conversions and with 34 and 84% *ee*, respectively (Table 1, entries 19 and 20). The best result obtained at room temperature employing ligand **17**[13,14] could not be ameliorated by lowering the reaction temperature to 0 ºC (Table 1, entry 21). In all of the examples depicted in Table 1 a total *endo*-selectivity was observed (^{1}H NMR of the crude mixture) except in the reaction promoted by phosphoramidite **14**.

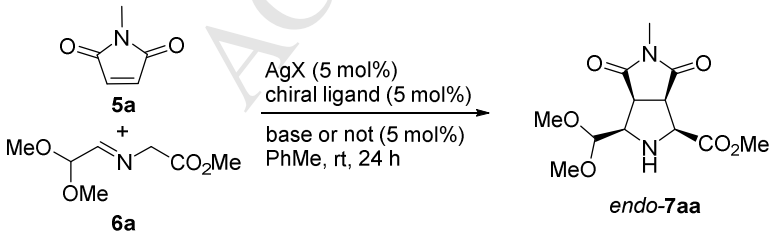

Scheme 1. Optimization of the enantioselective 1,3-DC of imine **6a** with NMM **5a**.

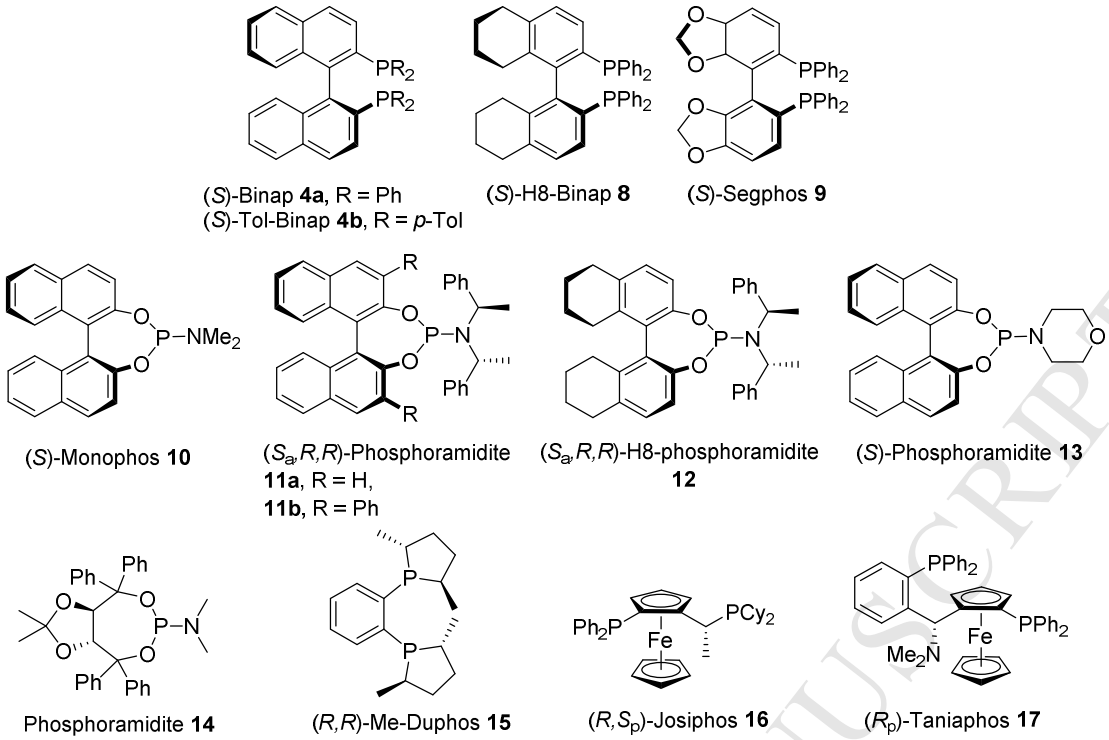

Figure 1. Ligands tested in the enantioselective 1,3-DC of **6a** and NMM **5a**.

Table 1. Optimization of the 1,3-DC of **6a** and **5a** to yield **7aa**.

Entry	Ligand	AgX	Base	Conv. (%)[a]	*ee* (%)[b]
1	(*S*)-BINAP **4a**	AgTfa	Et_3N	100	60
2	(*S*)-BINAP **4a**	AgTfa	DIPEA	100	60
3	(*S*)-BINAP **4a**	AgTfa	—	100	64
4	(*S*)-BINAP **4a**	Ag_2CO_3	—	100	60
5	(*S*)-BINAP **4a**	AgOAc	—	100	54
6	(*S*)-BINAP **4a**	AgOBz	—	100	65
7	(*S*)-BINAP **4a**	AgF	—	100	72
8	(*S*)-BINAP **4a**	AgF	—[c]	100	62
9	(*S*)-Tol-BINAP **4b**	AgF	—	100	72
10	(*S*)-H8-BINAP **8**	AgF	—	100	50
11	(*S*)-Segphos **9**	AgF	—	95	34
12	(*S*)-Monophos **10**	AgF	—	100	11
13	(S_a,*R*,*R*)-Phosphoramidite **11a**	AgF	—	100	20
14	(S_a,*R*,*R*)-Phosphoramidite **11b**	AgF	—	100	26
15	(S_a,*R*,*R*)-H8-Phosphoramidite **12**	AgF	—	100	62
16	(*S*)- Phosphoramidite **13**	AgF	—	100	4

17	Phosphoramidite **14**	AgF	—	100	60[d]
18	(*R*,*R*)-Me-Duphos **15**	AgF	—	90	6
19	(R,S_p)-Josiphos **16**	AgF	—	100	-34[e]
20	(R_p)-Taniaphos **17**	AgF	—	100	-84[e]
21	(R_p)-Taniaphos **17**	AgF	—[f]	100	-82[e]

[a] Determined by ^{1}H NMR of the crude reaction mixture.
[b] Determined by HPLC using chiral coated columns. Only *endo*-**7a** was identified by ^{1}H NMR of the crude reaction product. Negative sign means that the opposite enantiomer was obtained.
[c] Performed at -20 ºC.
[d] Mixture of *endo*/*exo*-diastereoisomers was detected.
[e] The opposite enantiomer was obtained.
[f] Performed at 0 ºC.

The (R_p)-Taniaphos **17**·AgF complex, prepared as previously described, was analyzed by ^{31}P NMR and electrospray ionization-mass spectrometry (ESI-MS). In the ^{31}P NMR experiment in deuterated chloroform no signals were observed between 25-150 ppm. The same behaviour was observed during the analysis of the catalyst generated form (S_a,*R*,*R*)-phosphoramidite **11a** and $AgClO_4$ employed in the study of the enantioselective 1,3-DCs of benzylideneamino esters and alkenes.[11] Thus, we propose that the normal polymeric character of these nitrogenated complexes is favored by π-interaction between an aromatic ring of the ligand and the silver atom.[11] In addition, acetonitrile/water mixtures employed during the ESI-MS were able to cleave this polymeric aggregation finding a molecular ion of *m/z* 794 corresponding to monomeric 1:1 ligand:silver atom species (R_p)-Taniaphos **17**·AgF (Figure 2). This disaggregation could also take place by the coordination of the freshly generated 1,3-dipole from imino ester **6a** to the silver atom, but ^{31}P NMR experiment did not clarify this idea.[11]

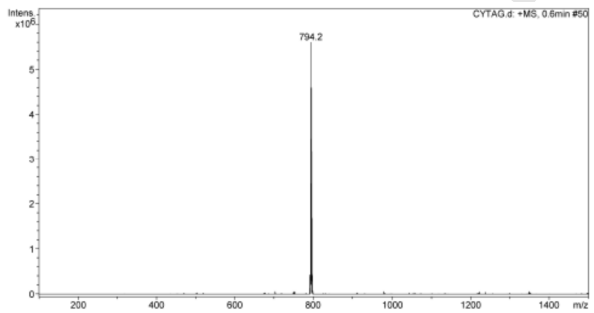

Figure 2. ESI-MS: *m/z* 794, [Taniaphos **17**· Ag]$^+$.

The scope of the optimized reaction conditions was extended to other different maleimides **5** and different imino esters **6** (Scheme 2). Imino ester **6a** (R^2 = H) reacted with *N*-alkylmaleimides, such as NMM (**5a**) and *N*-benzylmaleimide (**5b**) affording *endo*-cycloadducts **7aa** and **7ab**, respectively. In both cases the isolated purified chemical yield was moderate (45 and 50%) although the crude reaction products were pure enough to be used for further transformations is desired. The enantioselectivity was 84 and 88% *ee* in both the crude and purified samples, respectively. *N*-

Arylmaleimides **5c-h** behave similarly, and NPM (**5c**) gave the best purified chemical yield (60%) of this series, *endo*-**7ac** being isolated with a 94% *ee*. 4-Substituted *N*-arylmaleimides furnished *endo*-**7ad**, *endo*-**7ae**, and *endo*-**7af** in moderate yield (40%, 45%, and 55%, respectively) but the enantioselectivities were excellent (90-99% *ee*). The *N*-(4-acetylphenyl)maleimide **5d** induced the best enantioselection of this study (99% *ee*). *N*-(3-Chlorophenyl)maleimide **5g** gave the corresponding product *endo*-**7ag**, similar to the results generated from the 4-substituted aryl surrogates (45% yield and 88% *ee*). However, the most sterically hindered *N*-(2-methoxyphenyl)maleimide (**5h**) gave a low yield (48%) of *endo*-**7ah** product, but with notable 86% *ee*. Using maleimide **5i** as the dipolarophile in the cycloaddition with **6a** generated *endo*-**7ai** in 45% yield and moderate 52% enantioselection. Imino esters **6b** and **6c** derived from phenylalanine and leucine were allowed to react with NMM (**5a**) obtaining cycloadducts that were much more stable to purification conditions. High yields (81% and 95%) and enantioselections (92% and 90% *ee*) of *endo*-**7ba** and *endo*-**7ca**, respectively, were obtained (Scheme 2). Acrylates, nitrostyrene, α,β-unsaturated ketones, vinyl sulfones, fumarates, maleic anhydride, benzo- and naphthoquinone, and acrylamides were poor dipolarophiles in the reaction, resulting in no or very poor conversions to products.

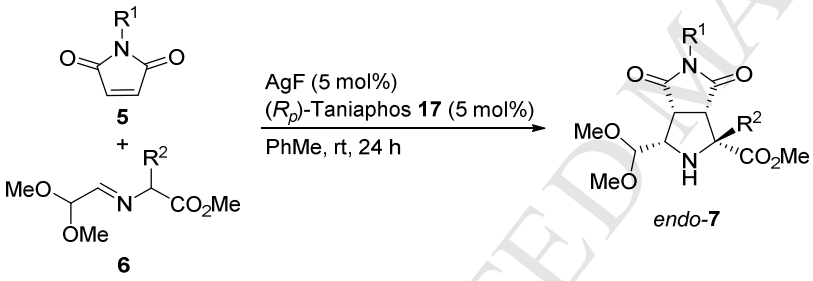

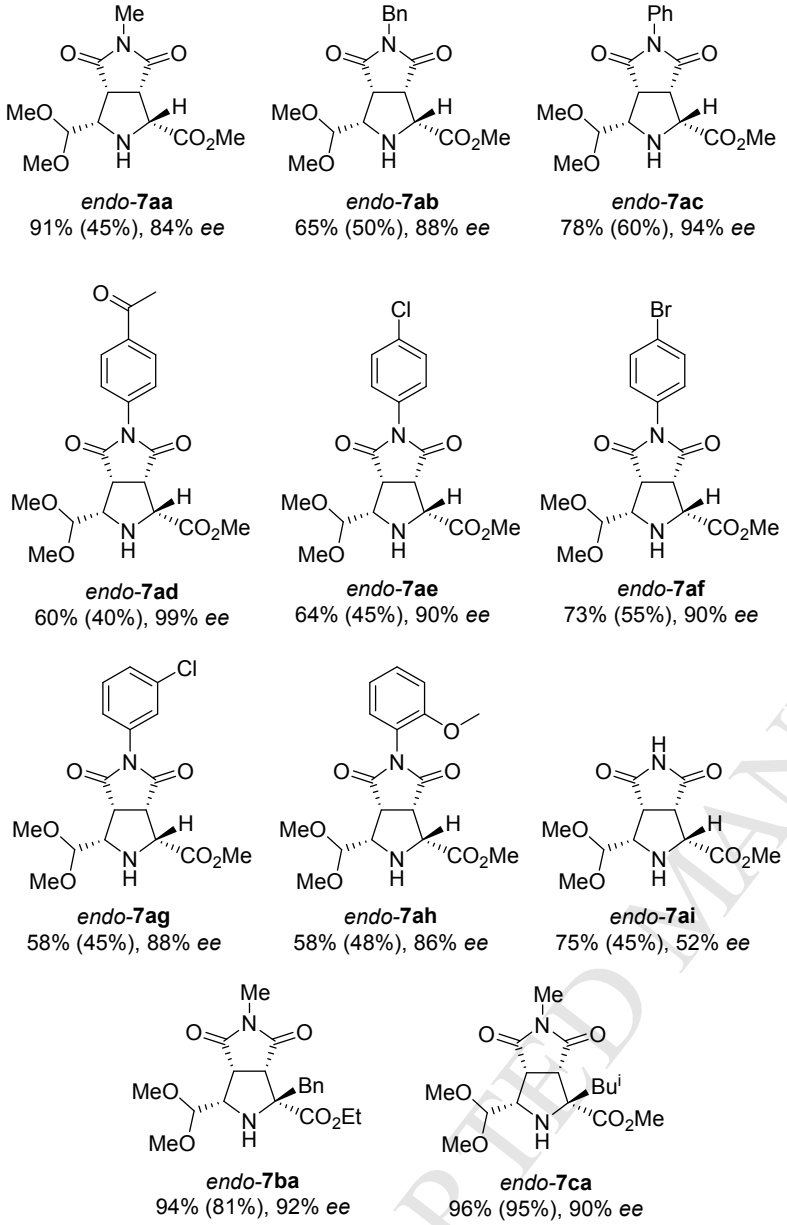

Scheme 2. Scope of the enantioselective 1,3-DC of imine **6** and NMM **5a**. In brackets are represented yields of purified compounds (flash chromatography).

In order to determine the absolute configuration of enantiomerically enriched products **7** their crystallization was attempted, but the crystals that were obtained were not suitable for X-ray diffraction analysis. In this sense, derivatization of molecules **7** was performed using methanosulfonyl or benzenesulfonyl chlorides in the presence of a base, but epimerization and some unidentified decomposition products were obtained. We therefore assigned the stereochemistry as indicated for **7aa** in Scheme 1 by analogy to that determined when using chiral BINAP **4a**·AgX[8,15,16] or by the chiral phosphoramidite **11a**·$AgClO_4$[11] in the 1,3-DCs between imino esters **18** and maleimides **5** (Scheme 3). According to the common preference of all these silver(I) complexes by the (1*S*,3*R*,3a*S*,6a*R*) configuration in compounds *endo*-**2** and *endo*-**19** it is reasonable

to propose this absolute configuration for the major enantiomer **7aa** identified in entries 1-15 of the Table 1.

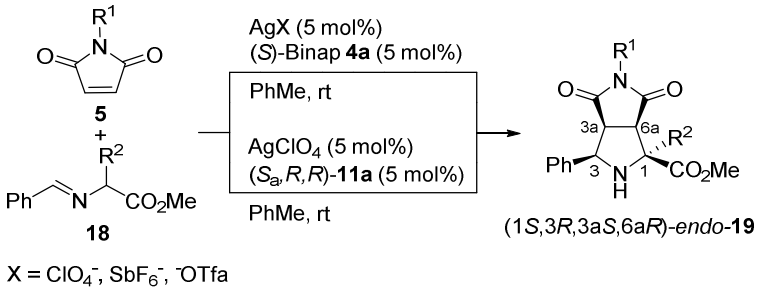

Scheme 3. Sterochemical outcome induced by (S_a)-BINAP **4a**·silver(I) salts[8,15,16] or phosphoramidite (S_a,*R*,*R*)-**11a**·$AgClO_4$[11] in the enantioselective silver-mediated 1,3-DCs of imine **18** and maleimides **5**.

Over the past years, DFT calculations have been shown to be a useful tool for the study of the enantioselectivity exhibited in 1,3-DCs catalyzed by chiral silver(I) complexes.[10b,11b,17] For that reason, we decided to perform a computational exploration of the Gibbs free energy profiles in order to analyze the different stereochemical outcomes observed when (*S*)-BINAP (**4a**) or (R_p)-Taniaphos (**17**) are used as chiral ligands (Table 1, entries 7 and 20).

In previous work, we demonstrated that the selectivity of the 1,3-DCs using chiral metallic complexes arises from the effective blockage of one of the prochiral faces.[18] Therefore, we started our study analyzing the main geometrical features of the azomethine ylides derived from imine **6a**. As reported in previous work describing 1,3-DC of azomethine ylides and and maleimides,[15b] it was stated that the fluoride counterion was not considered for calculations because of its long distance from the silver cation. Although ^{19}F NMR shifts are not a measure of the naked ness of fluoride[19] it is possible to use them to establish the relative strength or weakness of the Ag–F bond in the presence or absence of ligands. ^{19}F NMR of (R_p)-Taniaphos (**17**)·AgF in deuterated acetonitrile revealed a signal at -100.8 ppm. This result indicated a weaker silver-fluorine bond than the corresponding one of pure silver fluoride (-166.3 ppm).[19,20] The computed most stable *N*-metallated complexes are gathered in Figure 3.

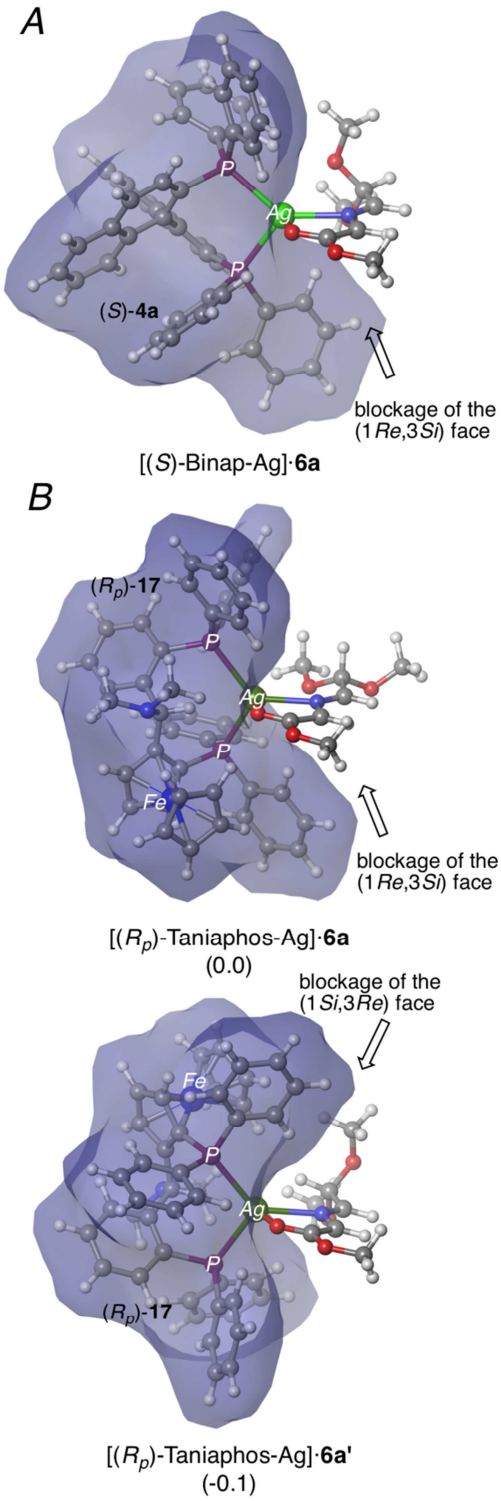

Figure 3. Main geometrical features and relative Gibbs free energies (in kcal mol^{-1} at 298K) of silver complexes derived from imine **6a** and (A) (*S*)-BINAP (**4a**) or (B) (R_p)-Taniaphos (**17**) computed at B3LYP/6-31G*&LANL2DZ level of theory. Blue surface represents the solvent-accessible surface with a probe radius of 1.9 Å.

Due to the C_2 symmetry of (*S*)-BINAP, only [(*S*)-BINAP-Ag]·**6a** was found as a minimum (Figure 3A). In this case, the metallic center is coordinated to the two phosphorous atoms of the ligand and to the oxygen of the enolate and the nitrogen atom of the azomethine ylide. This coordination pattern leads to the blockage of the (1*Re*,3*Si*) prochiral face by the phenyl groups of

one phosphine unit, thus prompting the formation of (1*S*,3*R*,3a*S*,6a*R*)-**7aa** cycloadducts (Scheme 2). On the other hand, when (R_p)-Taniaphos was considered as chiral ligand, two energetically accessible *N*-metallated azomethine ylides are found (Figure 3B). In both ylides, the two phosphorous atoms of the ligand are coordinated to the silver atom.[21] Therefore, the coordination pattern found for both chiral ligands agrees with the absence of signals corresponding to uncoordinated aromatic phosphines in the ^{31}P-NMR spectra (*vide supra*). Noteworthy, with this latter chiral ligand, all of the possible metallated complexes effectively block different prochiral faces by the diphenylphosphino group attached to the ferrocenyl group. However, the difference in energy between them is not enough to assume that only one of them was the real catalytic species in solution at room temperature. Therefore, further computational analysis is required for theoretically assess the stereochemical outcome.

We next proceeded to compute the complete profile associated with the 1,3-DCs of NMM (**5a**) and the above-described azomethine ylides. In previous work on 1,3-DCs-assisted by chiral Ag-based catalysts we have observed a clear preference for the formation of *endo*-cycloadducts.[22] This *endo* preference is consequence of an electrostatic interaction between the nitrogen atom of the maleimide and the silver atom. Also a closer distance of one methoxy group of the imino moiety and the silver atom exists ($d_{Ag\text{-}e}$ = 2.73-2.75Å for BINAP **4a** complex and $d_{Ag\text{-}e}$ = 2.76-2.94Å for Taniaphos **17** complex, Figure 4) was detected. Therefore, we only have considered the formation of cycloadducts *endo*-**7aa** and *ent-endo*-**7aa** via transition structures **TS1** and **TS2**, respectively.[23] The main geometrical features and relative Gibbs free energies of the least energetic transition structures are collected in Figure 4.

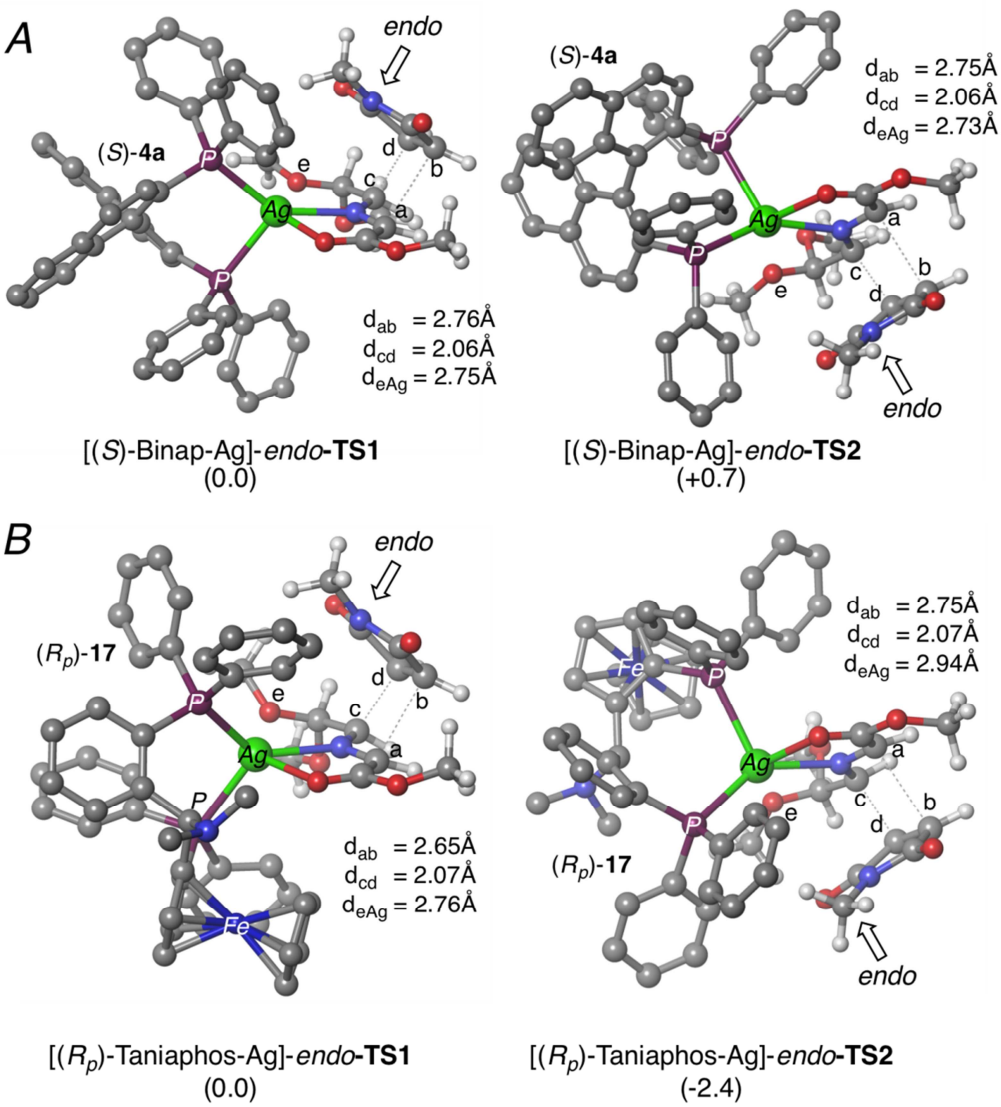

Figure 4. Main geometrical features and relative Gibbs free energies (in kcal mol^{-1} at 298K) of transition structures associated with the 1,3-DCs of NMM (**5a**) with silver complexes derived from imine **6a** and (A) (*S*)-BINAP (**4a**) or (B) (R_p)-Taniaphos (**17**) computed at B3LYP/6-31G*&LANL2DZ level of theory. Hydrogen atoms of the chiral ligands are omitted for clarity.

Our results show that lowest energy transition states **TS1** and **TS2** are concerted but quite asynchronous, the distance C(3)-C(3a) distance being shorter than its C(1)-C(6a) counterpart (d_{cd} and d_{ab} in Figure 4 respectively) as in previously reported calculations on similar systems.[11b] For the computed profile for the (*S*)-BINAP **4a**·Ag catalyzed 1,3-DC, **TS1** was found to be 0.7 kcal mol^{-1} more stable than **TS2** (Figure 4A). In the latter transition structure, a higher steric clash between the incoming dipolarophile **5a** and one phenyl group of (*S*)-BINAP was found, as expected after examination of [(*S*)-BINAP **4a** -Ag]·**6a** azomethine ylide (*vide supra*).

On the contrary, in the computed profile for the (R_p)-Taniaphos·Ag-catalyzed 1,3-DC, **TS2** was found to be 2.4 kcal mol^{-1} more stable than **TS1**, thus pointing out to the preferential formation of *endo*-**7aa** (Figure 4B). In this case the theoretical *endo*-**7aa**:*ent-endo*-**7a** ratio is obtained of 1:>99 due to the higher energetic gap between transition structures. Noteworthy, that result is in

great agreement with the experimental evidence. Remarkably, each transition structure is related to one of the previously computed (R_p)-Taniaphos·**6a** azomethine ylides, showing the effective blockage of the biphenylphosphine moiety attached to the ferrocenyl group advanced by the analysis of the initial azomethine ylides.

Finally, the Gibbs energy profiles associated with the computed catalytic cycles were computed (Scheme 4). Our results show that the computed activation barriers are low, confirming the high conversions and mild conditions described experimentally. Our results show, however, that (R_p)-Taniaphos **17**·Ag catalytic system present a slightly lower activation barrier associated with 1,3-DC step compared to (*S*)-BINAP **4a**·Ag. It is observed that the cycloaddition step is endothermic in both cases. However, the final step that recovers the catalyst is spontaneous, ensuring the recovery of the initial azomethine ylide by release of the final product by coordination of fresh imine to the metallic centre.

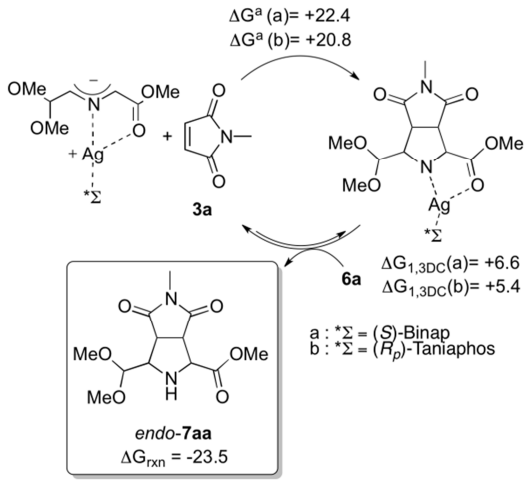

Scheme 4. Gibbs energy profile associated with the formation of cycloadduct 7aa catalyzed by silver and (a) (*S*)-BINAP (**4a**) or (b) (R_p)-Taniaphos (**17**) chiral ligand computed at B3LYP/6-31G*&LANL2DZ level of theory. Energies are in kcal mol^{-1} and computed at 298 K.

3. Conclusions

The first 1,3-DCs of maleimides and imino esters derived from 2,2-dimethoxyacetaldehyde was efficiently accomplished by the chiral catalyst (R_p)-Taniaphos·AgF, which was better than other chiral ligands tested under very mild reaction conditions. This catalyst can be defined as multifunctional because: a) it activates the dipole with a high control of its geometry; b) it can act as base accelerating the reaction; and c) it allows the approach of the maleimide through a weak N-Ag interaction. In all cases the reaction was *endo*-diastereoselective giving rise to 2,5-*cis*-arrangements between two reactive functional groups. Despite problems assigning the absolute configuration, experimental results and DFT calculations were used to confirm the proposed stereochemistry of *endo*-cycloadducts. DFT calculations also supported the different enantioselection observed when (R_p)-Taniaphos was used as a source of chirality in comparison with the analogous reaction mediated by the (*S*)-BINAP ligand.

4. Experimental Part

4.1. General information

Melting points were determined with a Reichert Thermowar hot plate apparatus and are uncorrected. Only the structurally most important peaks of the IR spectra (recorded whit a FT-IR 4100LE (JASCO) (PIKE MIRacle ATR) are listed. ^{1}H NMR (300 MHz) ^{13}C NMR (75 MHz) ^{31}P NMR (120 MHz) and spectra were obtained with a Bruker AC-300 by using $CDCl_3$ as solvent and TMS as the internal standard, unless otherwise stated. Optical rotations were measured with a Perkin-Elmer 341 polarimeter. HPLC analyses were performed with a JASCO-2000 series equipped with a chiral column (detailed for each compound in the main text) by using mixtures of *n*-hexane/isopropyl alcohol as the mobile phase at 25 ºC. Low-resolution electron impact (EI) mass spectra were obtained with a Shimadzu QP-5000 by injection or DIP, and high-resolution mass spectra were obtained with a Finnigan VG Platform or a Finnigan MAT 95S. Analytical TLC was performed on Schleicher & Schuell F1400/LS 254 silica gel plates and the spots were visualized under UV light (λ = 254 nm). Merck silica gel 60 (0.040-0.063 mm) was used for flash chromatography.

4.2. General procedure for the enantioselective 1,3-DCs.

In a 10 mL vial covered by aluminum foil, was added AgF (0.63 mg, 0.005 mmol), (R_p)-Taniaphos (3.44 mg, 0.005 mmol) and toluene (1 mL), and the resulting mixture was stirred at room temperature for 1 h. Dimethoxyacetaldehyde imine derivative **6** (0.1 mmol), the corresponding maleimide **5** (0.1 mmol) in toluene (2 mL) were added. After 1 d stirring at room temperature the crude was analyzed by ^{1}H NMR spectroscopy to determine the diastereomeric ratio, and then purified by column chromatography (flash silicagel) eluting with mixtures of hexane and ethyl acetate, affording the product *endo*-**7**.

4.3. Methyl (1*R*,3*S*,3a*R*,6a*S*)-3-(dimethoxymethyl)-5-methyl-4,6-dioxooctahydropyrrolo[3,4-*c*]pyrrole-1-carboxylate *endo*-7aa: Sticky pale yellow oil, 15 mg (45%); $[\alpha]_D^{25} = -14.5$ (*c* 0.25, $CHCl_3$), 84% *ee* from HPLC (Daicel Chiralpak OD-H), hexane/*i*-PrOH 60/40, flow rate 0.8 mL/min, t_{Rmin}: 25.6 min, t_{Rmaj}: 31.5 min, 254 nm; IR ν_{max}: 3648, 1747, 1697 cm^{-1}; ^{1}H-NMR δ: 2.14 (br. s, 1H, NH), 2.96 (s, 3H, MeN), 3.32 (t, *J* = 7.8 Hz, 1H, CHCHC*H*CON), 3.42 (s, 3H, CHO*Me*), 3.44-3.54 (m, 2H, C*H*CHCO$_2$Me, C*H*CHO$_2$), 3.55 (s, 3H, CHO*Me*), 3.84 (s, 3H, CO$_2$Me), 3.98 (d, *J* = 7.8 Hz, 1H, C*H*CO$_2$Me), 4.70 (d, *J* = 4.6 Hz, 1H, CHO$_2$); ^{13}C-NMR δ: 25.2 (NCH$_3$), 46.4, 49.1 (2xCHCON), 52.5 (CO$_2$*Me*), 55.8, 56.0 (2xCO*Me*), 62.1 (*C*HCO$_2$Me), 63.4 (*C*HCHO$_2$), 102.7 (CHO$_2$), 170.0, 175.7, 175.8 (3xCO); MS *m/z* (%): 286 (M$^+$ 1%), 211 (16), 195 (30), 165 (22), 151 (15), 94 (18), 75 (100); HRMS calculated for ($C_{12}H_{18}N_2O_6$): 286.1165, found: 286.1158.

4.4. Methyl (1*R*,3*S*,3a*R*,6a*S*)-5-benzyl-3-(dimethoxymethyl)-4,6-dioxooctahydropyrrolo[3,4-*c*]pyrrole-1-carboxylate *endo*-7ab: Sticky colourless oil, 18 mg (50%); $[\alpha]_D^{25} = -23.8$ (*c* 1.18, $CHCl_3$), 88% *ee* from HPLC (Daicel Chiralpak IA), hexane/*i*-PrOH 90/10, flow rate 1 mL/min, t_{Rmaj}: 23.1 min, t_{Rmin}: 24.9 min, 254 nm; IR ν_{max}: 3656, 1747, 1700 cm^{-1}; ^{1}H-NMR δ: 2.10 (br. s, 1H, NH); 3.17 (s, 3H, CHO*Me*), 3.31 (dd, *J* = 8.3, 2.8, 1H, CHCHC*H*CON), 3.49 (s, 3H, CHO*Me*), 3.72-3.80 (m, 2H, C*H*CHCO$_2$Me, C*H*CHO$_2$), 3.83 (s, 3H, CO$_2$Me), 3.99 (d, *J* = 7.7 Hz, 1H, C*H*CO$_2$Me), 4.55 (d, *J* = 14.3 Hz, 1H, CH$_2$), 4.65-4.73 (m, 2H, 1H CH$_2$, CHO$_2$), 7.29-7.38 (m, 5H, Ar*H*); ^{13}C-NMR δ: 42.9 (CH$_2$), 46.6, 49.3 (2x*C*HCON), 52.6 (CO$_2$*Me*), 55.6, 55.8 (2xCO*Me*), 62.4 (*C*HCO$_2$Me), 63.7 (*C*HCHO$_2$), 102.0 (CHO$_2$), 128.0, 128.6, 128.7, 135.5 (Ar*C*), 169.6, 175.2, 175.3 (3xCO); MS *m/z* (%): 362 (M$^+$ 1%), 300 (15), 287 (20), 271 (17), 241 (19), 227 (15), 91 (35), 75 (100); HRMS calculated for ($C_{18}H_{22}N_2O_6$): 362.1478, found: 362.1465.

4.5. Methyl (1*R*,3*S*,3a*R*,6a*S*)-3-(dimethoxymethyl)-4,6-dioxo-5-phenyloctahydropyrrolo[3,4-*c*]pyrrole-1-carboxylate *endo*-7ac: Sticky colourless oil, 21 mg (60%); $[\alpha]_D^{25} = -33.1$ (*c* 0.86, $CHCl_3$), 94% *ee* from HPLC (Daicel Chiralpak OD-H), hexane/*i*-PrOH 60/40, flow rate 0.8 mL/min, t_{Rmaj}: 24.9 min, t_{Rmin}: 31.7 min, 254 nm; IR ν_{max}: 3748, 1746, 1705 cm^{-1}; ^{1}H-NMR δ: 2.13 (br. s, 1H, NH); 3.40 (s, 3H, CHO*Me*), 3.44-3.50 (m, 2H, CHCHC*H*CON, C*H*CHO$_2$), 3.55 (s, 3H, CHO*Me*), 3.68 (t, *J* = 7.8 Hz, 1H, C*H*CHCO$_2$Me), 3.83 (s, 3H, CHO*Me*), 4.12 (d, *J* = 7.8 Hz, 1H, C*H*CO$_2$Me), 4.80 (d, *J* = 3.7 Hz, 1H, CHO$_2$), 7.21-7.26 (m, 2H, Ar*H*), 7.35-7.50 (m, 3H, Ar*H*); ^{13}C-NMR δ: 46.9, 49.4 (2x*C*HCON), 52.7 (CO$_2$*Me*), 56.0, 56.1

(2xCO*Me*), 62.6 (*C*HCO$_2$Me), 64.0 (*C*HCHO$_2$), 102.1 (CHO$_2$), 126.7, 129.0, 129.3, 131.8 (Ar*C*), 169.8, 174.7, 174.8 (3xCO); MS (EI) *m/z* (%): 348 (M$^+$ 1%), 286 (15), 273 (16), 257 (22), 227 (30), 94 (19), 75 (100); HRMS calculated for ($C_{17}H_{20}N_2O_6$-$C_3H_7O_2$): 273.0875, found: 273.0873.

4.6. Methyl (1*R*,3*S*,3a*R*,6a*S*)-5-(4-acetylphenyl)-3-(dimethoxymethyl)-4,6-dioxooctahydropyrrolo[3,4-*c*]pyrrole-1-carboxylate *endo*-7ad: Colourless oil, 16 mg (40%); $[\alpha]_D^{25}$ = -26.3 (*c* 0.49, $CHCl_3$), 99% *ee* from HPLC (Daicel Chiralpak ADH), hexane/*i*-PrOH 90/10, flow rate 1 mL/min, t_{Rmaj}: 17.7 min, t_{Rmin}: 21.8 min, 254 nm; IR ν_{max}: 3674, 1743, 1703, 1683 cm^{-1}; ^{1}H-NMR δ: 2.62 (s, 3H, MeC=O), 3.10 (br. s, 1H, NH); 3.39 (s, 3H, CHO*Me*), 3.42-3.49 (m, 1H, CHCHC*H*CON), 3.55 (s, 3H, CHO*Me*), 3.64 (dd, *J* = 8.3, 3.5 Hz, 1H, C*H*CHO$_2$), 3.72 (td, *J* = 7.5, 4.5, 1H, C*H*CHCO$_2$Me), 3.84 (s, 3H, OMe), 4,13 (d, *J* = 7.5, 1H, C*H*CO$_2$Me), 4.79 (d, *J* = 3.5 Hz, 1H, CHO$_2$), 7.40, 8,05 (2xd, *J* = 8.3 Hz, 4H, Ar*H*); ^{13}C-NMR δ: 26.8 (*Me*C=O), 46.8, 49.4 (2x*C*HCON), 52.8 (CO$_2$*Me*), 55.9, 56.0 (2xCO*Me*), 62.5 (*C*HCO$_2$Me), 63.9 (*C*HCHO$_2$), 102.0 (CHO$_2$), 126.6, 129.3, 135.8, 137.0 (Ar*C*), 169.9, 174.2, 174.2 (3xCO), 197.1 (Me*C*=O); MS (EI) *m/z* (%): 390 (M$^+$ 1%), 299 (8), 146 (5), 126 (4), 94 (8), 84 (5), 75 (100), 68 (5); HRMS calculated for ($C_{19}H_{22}N_2O_7$-$C_3H_7O_2$): 315.0981, found: 315.0965.

Methyl (1*R*,3*S*,3a*R*,6a*S*)-5-(4-chlorophenyl)-3-(dimethoxymethyl)-4,6-dioxooctahydropyrrolo[3,4-*c*]pyrrole-1-carboxylate *endo*-7ae: Pale yellow oil, 18 mg (45%); $[\alpha]_D^{25}$ = -50.1 (*c* 0.66, $CHCl_3$), 90% *ee* from HPLC (Daicel Chiralpak ODH), hexane/*i*-PrOH 60/40, flow rate 0.8 mL/min, t_{Rmaj}: 27.8 min, t_{Rmin}: 35.3 min, 254 nm; IR ν_{max}: 3675, 1746, 1707 cm^{-1}; ^{1}H-NMR δ: 2.65 (br. s, 1H, NH); 3.39 (s, 3H, CHO*Me*), 3.44-3.51 (m, 1H, CHCHC*H*CON), 3.54 (s, 3H, CHO*Me*), 3.60 (dd, *J* = 8.3, 4.10 Hz, 1H, C*H*CHO$_2$), 3.69 (t, *J* = 7.8, 1H, C*H*CHCO$_2$Me), 3.83 (s, 3H, CO$_2$Me), 4.07 (d, *J* = 7.8 Hz, 1H, C*H*CO$_2$Me), 4.77 (d, *J* = 4.0 Hz, 1H, CHO$_2$), 7.21, 7.43 (2xd, *J* = 8.9 Hz, 4H, Ar*H*); ^{13}C-NMR δ: 46.8, 49.4 (2x*C*HCON), 52.7 (CO$_2$*Me*), 55.9, 56.0 (2xCO*Me*), 62.6 (*C*HCO$_2$Me), 64.0 (*C*HCHO$_2$), 102.1 (CHO$_2$), 127.9, 129.5, 130.2, 134.8 (Ar*C*), 169.8, 174.5, 174.5 (3xCO); MS (EI) *m/z* (%): 382 (M$^+$ 1%), 320 (15), 291 (15), 261 (36), 153 (14), 94 (14), 75 (100); HRMS calculated for ($C_{17}H_{19}ClN_2O_6$-ClC_6H_4): 271.0930, found: 271.0939.

Methyl (1*R*,3*S*,3a*R*,6a*S*)-5-(4-bromophenyl)-3-(dimethoxymethyl)-4,6-dioxooctahydropyrrolo[3,4-*c*]pyrrole-1-carboxylate *endo*-7af: Colourless oil, 23 mg (53%); $[\alpha]_D^{25}$ = -44.7 (*c* 0.98, $CHCl_3$), 90% *ee*, from HPLC (Daicel Chiralpak ODH), hexane/*i*-PrOH 60/40, flow rate 0.8 mL/min, t_{Rmaj}: 29.8 min, t_{Rmin}: 36.9 min, 254 nm; IR ν_{max}: 3656, 1752, 1710 cm^{-1}; H-NMR δ: 3.38 (s, 3H, CHO*Me*), 3.43-3.51 (m, 2H, NH, CHCHC*H*CON), 3.54 (s, 3H, CHO*Me*), 3.59-3.61 (m, 1H, C*H*CHO$_2$), 3.67-3.79 (m, 1H, C*H*CHCO$_2$Me), 3.83 (s, 3H, CO$_2$Me), 4.10 (d, *J* = 7.8 Hz, 1H, C*H*CO$_2$Me), 4.78 (d, *J* = 3.9 Hz, 1H, CHO$_2$), 7.15 (d, *J* = 8.8 Hz, 2H, Ar*H*), 7.59 (d, *J* = 8.8 Hz, 2H, Ar*H*); ^{13}C-NMR δ: 46.8, 49.3 (2x*C*HCON), 52.8 (CO$_2$*Me*), 55.9, 56.0 (2xCO*Me*), 62.6 (*C*HCO$_2$Me), 63.9 (*C*HCHO$_2$), 102.0 (CHO$_2$), 122.8, 128.2, 130.6, 132.5 (Ar*C*), 169.7, 174.4, 174.5 (3xCO); EM (IE) *m/z* (%):427 (M$^+$ 1%), 395 (5), 335 (7), 307 (7), 197 (6), 110 (5), 94 (13%), 75 (100); HRMS calculated for ($C_{17}H_{19}BrN_2O_6$-$C_3H_7O_2$): 350.9980, found: 350.9979.

Methyl (1*R*,3*S*,3a*R*,6a*S*)-5-(3-chlorophenyl)-3-(dimethoxymethyl)-4,6-dioxooctahydropyrrolo[3,4-*c*]pyrrole-1-carboxylate *endo*-7ag: Pale yellow oil, 18 mg (45%); $[\alpha]_D^{25}$ = -48.4 (*c* 0.62, $CHCl_3$) 88% *ee*, from HPLC (Daicel Chiralpak ODH), hexane/*i*-PrOH 60/40, flow rate 0.8 mL/min, t_{Rmaj}: 23.8 min, t_{Rmin}: 30.1 min, 254 nm; IR ν_{max}: 3675, 1746, 1713 cm^{-1}; ^{1}H-NMR δ: 3.41 (s, 3H, CHO*Me*), 3.44-3.51 (m, 2H, NH, CHCHC*H*CON), 3.55 (s, 3H, CHO*Me*), 3.68-3.81 (m, 2H, C*H*CHCO$_2$Me, C*H*CHO$_2$), 3.85 (s, 3H, CO$_2$Me), 4.17 (d, *J* = 7.8 Hz, 1H, C*H*CO$_2$Me), 4.80 (d, *J* = 3.8 Hz, 1H, CHO$_2$), 7.15-7.20 (m, 1H, Ar*H*), 7.28-7.30 (m, 1H, Ar*H*), 7.35-7.45 (m, 2H, Ar*H*); ^{13}C-NMR δ: 46.7, 49.3 (2x*C*HCON), 52.9 (CO$_2$*Me*), 56.1, 56.2 (2xCO*Me*), 62.4 (*C*HCO$_2$Me), 63.8 (*C*HCHO$_2$), 101.8 (CHO$_2$), 124.8, 126.9, 129.2, 130.3, 132.8, 134.8 (Ar*C*), 169.4, 174.1, 174.2 (3xCO); MS (EI) *m/z* (%): 382 (M$^+$ 1%), 320 (15), 291 (13), 261 (28), 153 (10), 94 (15), 75 (100); HRMS calculated for ($C_{17}H_{19}ClN_2O_6$-$C_3H_7O_2$): 307.0486, found: 307.0479.

Methyl (1*R*,3*S*,3a*R*,6a*S*)-3-(dimethoxymethyl)-5-(2-methoxyphenyl)-4,6-dioxooctahydropyrrolo[3,4-*c*]pyrrole-1-carboxylate *endo*-7ah: Pale yellow oil, 10 mg (25%); $[\alpha]_D^{25}$ = -18.4 (*c* 0.36, $CHCl_3$) 86% *ee*, from HPLC (Daicel Chiralpak ODH), hexane/*i*-PrOH 60/40, flow rate 0.8 mL/min, t_{Rmaj}: 23.1 min, t_{Rmin}: 36.7 min, 254 nm; IR ν_{max}: 3751, 1746, 1709 cm^{-1}; ^{1}H-NMR δ: 3.34 (s, 3H, CHO*Me* $_{min}$); 3.43 (s, 3H, CHO*Me*);

3.44-3.50 (m, 6H, NH, CHCHC*H*CON, C*H*CHCO$_2$Me), 3.52 (s, 3H, CHO*Me*$_{min}$), 3.55 (s, 3H, CHO*Me*), 3.66-3.77 (m, 2H, C*H*CHO$_2$), 3.78 (s, 3H, CHO*Me*), 3.81 (s, 3H, ArO*Me*$_{min}$, ArO*Me*), 3.82 (s, 3H, CO$_2$Me), 3.86 (s, 3H, CO$_2$Me$_{min}$), 4.16 (t, *J* = 7.2 Hz, 1H, C*H*CO$_2$Me), 4.75 (d, *J* = 4.4 Hz, 1H$_{min}$, CHO$_2$), 4.83 (d, *J* = 3.8, 1H, CHO$_2$), 6.97-7.05 (m, 4H, Ar*H*), 7.11 (ddd, *J* = 8.0, 6.2, 1.7, 2H, Ar*H*), 7.36-7.42 (m, 2H, Ar*H*); ^{13}C-NMR δ: 46.9, 47.3, 49.4, 49.5 (4x*C*HCON), 52.6, 52.8, 55.2, 55.8, 55.9, 56.0 (6xOMe), 62.3, 62.7 (2x*C*HCO$_2$Me), 63.6, 63.8 (2x*C*HCHO$_2$), 101.8, 101.9 (2xCHO$_2$), 112.1, 112.3, 120.4, 120.7, 120.9, 121.1, 129.0, 129.4, 130.9, 131.2, 154.3, 154.7 (Ar*C*), 169.1, 161.2, 169.5, 174.2, 174.3, 174.4 (6xCO); MS (EI) *m/z* (%): 378 (M$^+$ 1%), 346 (15), 315 (17), 303 (62), 287 (31), 257 (15), 149 (21), 110 (16), 94 (38), 75 (100); HRMS calculated for ($C_{18}H_{22}N_2O_7$): 378.1427, found: 378.1423.

Methyl (1*R*,3*S*,3a*R*,6a*S*)-3-(dimethoxymethyl)-4,6-dioxooctahydropyrrolo[3,4-*c*]pyrrole-1-carboxylate *endo*-7ai: Pale yellow oil, 14 mg (45%); $[\alpha]_D^{25} = -17.8$ (*c* 0.35, $CHCl_3$) 52% *ee*, from HPLC (Daicel Chiralpak ODH), hexane/*i*-PrOH 60/40, flow rate 0.8 mL/min, t_{Rmin}: 18.2 min, t_{Rmaj}: 23.2 min, 254 nm; IR ν_{max}: 3800-3650, 1740, 1709 cm^{-1}; ^{1}H-NMR δ: 1.75-2.5 (br. S, 2H, 2xNH), 3.34 (t, *J* = 8.0 Hz, 1H, CHCHC*H*CON), 3.44 (s, 3H, CHO*Me*), 3.48 (dd, *J* = 9.1, 4.7 Hz, 1H, C*H*CHO$_2$), 3.54 (s, 3H, CHO*Me*), 3.58 (t, *J* = 8.0, Hz, 1H, C*H*CHCO$_2$Me), 3.83 (s, 3H, CO$_2$Me), 3.97 (d, *J* = 7.9 Hz, 1H, C*H*CO$_2$Me), 4.71 (d, *J* = 4.7 Hz, 1H, CHO$_2$); ^{13}C-NMR δ: 47.5, 50.1 (2x*C*HCON), 52.8, 55.9 (2xCHO*Me*), 56.1 (CO$_2$*Me*), 61.9 (*C*HCO$_2$Me), 63.3 (*C*HCHO$_2$), 102.2 (CHO$_2$), 169.1, 174.9, 175.0 (3xCO); MS (EI) *m/z* (%): 272 (M$^+$ 1%), 241 (15), 181 (24), 151 (18), 94 (14), 75 (100); HRMS calculated for ($C_{11}H_{16}N_2O_6$-$C_3H_7O_2$): 197.0562, found: 197.0570.

Methyl (1*R*,3*S*,3a*R*,6a*S*)-1-benzyl-3-(dimethoxymethyl)-5-methyl-4,6-dioxooctahydropyrrolo[3,4-*c*]pyrrole-1-carboxylate *endo*-7ba: Pale yellow oil, 32 mg (81%); $[\alpha]_D^{25} = -21.4$ (*c* 1.43, $CHCl_3$) 92% *ee*, from HPLC (Daicel Chiralpak ODH), hexane/*i*-PrOH 95/5, flow rate 1 mL/min, t_{Rmaj}: 34.1 min, t_{Rmin}: 39.4 min, 254 nm; IR ν_{max}: 3659, 1726, 1698 cm^{-1}; ^{1}H-NMR δ: 1.34 (t, *J* = 7.2 Hz, 3H, CCH$_3$), 2.93 (s, 3H, MeN), 3.02 (br. s, Hz, 1H, NH), 3.27-3.46 (m with s at 3.35, 7H, 2xCHCON, C*H*$_2$Ph, OMe), 3.49 (s, 3H, OMe), 3.71 (dd, *J* = 8.5, 3.5 Hz, 1H, C*H*CHO$_2$), 4.27 (qd, *J* = 7.1, 1.0 Hz, 2H, C*H*$_2$Me), 4.67 (d, *J* = 3.9 Hz, 1H, CHO$_2$), 7.27 (m, 5H, Ar*H*); ^{13}C-NMR δ: 14.2 (CH$_2$*C*H$_3$), 25.2 (NCH$_3$), 40.9 (*C*H$_2$Ar), 47.0, 55.0 (2x*C*HCON), 55.7, 55.7 (2xCHO*Me*), 61.5 (*C*HCO$_2$Me), 62.0 (*C*HCHO$_2$), 72.2 (*C*CH$_2$Ph), 102.1 (CHO$_2$), 127.3, 128.5, 130.2, 135.7 (Ar*C*), 170.6, 175.3, 175.8 (3xCO); MS (EI) *m/z* (%): 390 (M$^+$ 1%), 315 (24), 299 (24), 285 (22), 267 (100), 237 (13), 91 (34), 75 (23); HRMS calculated for ($C_{20}H_{26}N_2O_6$-$C_3H_7O_2$): 315.1345, found: 315.1347.

Methyl (1*R*,3*S*,3a*R*,6a*S*)-1-(2-methylpropyl)-3-(dimethoxymethyl)-5-methyl-4,6-dioxooctahydropyrrolo[3,4-*c*]pyrrole-1-carboxylate *endo*-7ca: Colourless sticky oil, 34 mg (95%); $[\alpha]_D^{25} = -18.5$ (*c* 1.33, $CHCl_3$) 90% *ee*, from HPLC (Daicel Chiralpak IA), hexane/EtOH 90/10, flow rate 1 mL/min, t_{Rmin}: 11.8 min, t_{Rmaj}: 18.5 min, 254 nm; IR ν_{max}: 3820-3650, 1734, 1698 cm^{-1}; ^{1}H-NMR δ: 0.83, 0.95 (2xd, *J* = 6.7 Hz, 6H, CH*Me*$_2$), 1.48 (dd, *J* = 14.2, 5.0 Hz, 1H, CH$_2$), 1.66-1.82 (m, 1H, C*H*Me$_2$), 1.99 (dd, 1H, *J* = 14.2, 9.0 Hz), 2.91 (s, 3H, NMe), 2.95 (br. s, Hz, 1H, NH), 3.12 (d, *J* = 7.6 Hz, 1H, CHCCO$_2$Me), 3,29 (dd, *J* = 7.6, 7.5 Hz, 1H, CHCHC*H*CON), 3.35, 3.47 (2xs, 6H, 2xCHO*Me*), 3.53 (dd, *J* = 7,5, 2.5 Hz, 1H, C*H*CHO$_2$), 3.83 (s, 3H, CO$_2$Me), 4.78 (d, *J* = 2.5 Hz, 1H, CHO$_2$); ^{13}C-NMR δ: 22.3, 24.2 (CH*Me*$_2$), 24.9 (CH$_2$), 25.1 (NCH$_3$), 43.7 (C*H*Me$_2$), 47.7, 52.5 (2x*C*HCON), 54.5, 55.7 (2xCHO*Me*), 57.3, 62.2, 71.4 (*C*CH$_2$CH), 100.9 (CHO$_2$), 172.5, 175.6, 176.2 (3xCO); MS (EI) *m/z* (%): 342 (M$^+$ 1%), 283 (35), 268 (15), 267 (100), 253 (15), 251 (24), 207 (43), 165 (25), 75 (89); HRMS calculated for ($C_{16}H_{26}N_2O_6$-$C_3H_7O_2$): 267.1345, found: 267.1349.

Acknowledgements: Financial support was provided by the Spanish Ministerio de Ciencia e Innovación (MICINN) (projects CTQ2010-20387, and Consolider Ingenio 2010, CSD2007-00006), the Spanish Ministerio de Economía y Competitividad (MINECO) (projects CTQ2013-43446-P, and CTQ2014-51912-REDC), FEDER, the Generalitat Valenciana (PROMETEO 2009/039 and PROMETEOII/2014/017), the University of Alicante, the Gobierno Vasco/Eusko Jaurlaritza (Grant IT673-13), and the Univeristy of the Basque Country UPV/EHU (UFI11/22 QOSYC). The SGI/IZO-SGIker and DIPC are gratefully thanked for generous allocation of computational resources.

References

1. Clovis J. S.; Eckell A.; Huisgen R.; Sustmann, R. *Chem. Ber*. **1967**, *100*, 60-70.
2. a) *Synthetic Applications of 1,3-Dipolar Cycloaddition Chemistry Toward Heterocycles and Natural Products*, Padwa, A.; Pearson, W. H. Eds., John Wiley & Sons: New Jersey, **2003**; b) Nájera, C.; Sansano, J. M. *Curr. Org. Chem*. **2003**, *7*, 1105-1150; c) Eberbach, W. In *Sci. Synth., Houben-Weyl Methods of Molecular Transformations*; Padwa, A., Bellus, D., Eds.; Thieme Verlag: Stuttgart, 2004; Vol. 27, chp. 11, pp 441-498; d) Coldham, I.; Hufton, R. *Chem. Rev*. **2005**, *105*, 2765-2810; e) Nair, V.; Suja, T. D. *Tetrahedron* **2007**, *63*, 12247-12275; f) Padwa, A.; Bur, S. K. *Tetrahedron* **2007**, *63*, 5341-5378; g) Hashimoto, T.; Maruoka, K. *Handbook of Cyclization Reactions*, Ma, S. Ed. Wiley-VCH: Weinheim, 2010; h) Kanemasa, S. *Heterocycles* **2010**, *82*, 87-200; i) Han, M.-Y.; Jia, J.-Y.; Wang, W. *Tetrahedron Lett.* **2014**, *55*, 784-794; j) Suga, H.; Itoh, K. in *Methods and Applications of Cycloaddition Reactions in Organic Syntheses*, Nishiwaki, N. Ed., Wiley: Weinheim, 2014, pp. 175-204.
3. For recent reviews of asymmetric 1,3-DC, see: a) Pellissier, H. *Tetrahedron* **2007**, *63*, 3235-3285; b) Nájera, C.; Sansano J. M. in *Topics in Heterocyclic Chemistry*, Hassner, A. Ed., Springer-Verlag: Berlin-Heidelberg, 2008, vol. 12, pp. 117-145; c) Stanley, L. M.; Sibi, M. P. *Chem. Rev.* **2008**, *108*, 2887-2902; d) Álvarez-Corral, M.; Muñoz-Dorado, M.; Rodríguez-García, I. *Chem. Rev*. **2008**, *108*, 3174-3198; e) Naodovic, M.; Yamamoto, H. *Chem. Rev*. **2008**, *108*, 3132-3148; f) Nájera, C.; Sansano, J. M.; Yus, M. *J. Braz. Chem. Soc.* **2010**, *21*, 377-412; g) Kissane, M.; Maguire, A. R. *Chem. Soc. Rev*. **2010**, *39*, 845-883; h) Adrio, J.; Carretero, J. C. *Chem. Commun*. **2011**, *47*, 6784-6794; i) Adrio, J.; Carretero, J. C. *Chem. Commun.*, **2014**, *50*, 12434-12446; j) Nájera, C.; Sansano, J. M. *J. Organomet. Chem*. **2014**, *771*, 78-92; k) Hashimoto, T.; Maruoka, K. *Chem. Rev.* **2015**, *115*, 5366-5412.
4. a) McCormack, M. P.; Shalumova, T.; Tanski, J. M.; Waters, S. P. *Org. Lett.* **2010**, *12*, 3906-3909; b) Machamer, N. K.; Liu, X.; Waters, S. P. *Org. Lett.* **2014**, *16*, 4996-4999.
5. Mancebo-Aracil, J.; Nájera, C.; Sansano, J. M. *Tetrahedron: Asymmetry* **2015,** *26*, 674-678; *Synfacts* **2015**, *11*, 1065
6. Mancebo-Aracil, J.; Cayuelas, A.; Nájera, C.; Sansano, J. M. *Tetrahedron* **2015**, *71*, 8804-8816.
7. a) *Privileged Chiral Ligands and Catalysts*, Qi-Lin Zhou, Ed.; Wiley-VCH: New York, 2011; b) J. F. Teichert, B. L. Feringa, *Angew. Chem. Int. Ed.* **2010**, *49*, 2486–2528.
8. Selection done according to the experience gained with this type of catalytic enantioselective 1,3-DC: Nájera, C.; Sansano, J. M. *Chem. Rec*. **2016**, in press.
9. Martín-Rodríguez, M.; Nájera, C.; Sansano, J. M.; Wu, F.-L. *Tetrahedron: Asymmetry* **2010**, *21*, 1184-1886; b) Martín–Rodríguez, M.; Nájera, C.; Sansano, J. M.; de Cózar, A.; Cossío, F. P. *Chem. Eur. J.* **2011**, *17*, 14224–14233.
10. Fluoride ion is the most basic of the halide anions in fact, hydrogen fluoride is a weak acid in water (pK_a = 3.18 in aqueous solution).
11. a) Nájera, C.; Retamosa, M. G.; Sansano, J. M. *Angew. Chem. Int. Ed.* **2008**, *47*, 6055-6058; b) Nájera, C.; Retamosa, M. G.; Martín-Rodríguez, M.; Sansano, J. M.; de Cózar, A.; Cossío, F. P. *Eur. J. Org. Chem.* **2009**, 5622-5634.
12. a) Castelló, L. M.; Nájera, C.; Sansano, J. M.; Larrañaga, O.; de Cózar, A.; Cossío, F. P. *Org. Lett.* **2013**, *15*, 2902-2905; b) Castelló, L. M.; Nájera, C.; Sansano, J. M.; Larrañaga, O.; de Cózar, A.; Cossío, F. P. *Adv. Synth. Catal.* **2014**, *356*, 3861-3870; c) Castelló, L. M.; Nájera, C.; Sansano, J. M.; Larrañaga, O.; de Cózar, A.; Cossío, F. P. *Synthesis* **2015**, *47*, 934-943.
13. Wheeler, P. In *e-EROS Encyclopedia of Reagents for Organic Synthesis*, Published online: 15 MAR 2012, DOI: 10.1002/047084289X.rn01449.
14. The enantiomer (S_p)-Taniaphos **17** is also commercially available.
15. a) Nájera, C.; Retamosa, M. G.; Sansano, J. M. *Org. Lett.* **2007**, *9*, 4025–4028; b) Nájera, C.; Retamosa, M. G.; Sansano, J. M.; de Cózar, A.; Cossío, F. P. *Tetrahedron*: *Asymmetry* **2008**, *19*, 2913-2923.
16. a) Martín-Rodríguez, M.; Nájera, C.; Sansano, J. M.; Costa, P. R. R.; Crizanto de Lima, E.; Dias, A. G. *Synlett* **2010,** 962-966; b) Mancebo-Aracil, J.; Martín-Rodríguez, M.; Nájera, C.; Sansano, J. M.; Costa, P. R. R.; Crizanto de Lima, E.; Dias, A. G. *Tetrahedron: Asymmetry* **2012**, *23*, 1596-1606.
17 Nájera, C.; Retamosa, M. G.; Sansano, J. M.; de Cózar, A.; Cossío, F. P. *Eur. J. Org. Chem* **2007**, 5038-5049.
18. De Cózar, A.; Cossío, F. P. *Phys. Chem. Chem. Phys.* **2011**, *13*, 10858-10868.
19. ^{19}F NMR shift of AgF in deuterated acetonitrile showed a signal at -166.3 ppm. Christe, K. O. Wilson, W. W. *J. Fluorine Chem.* **1990**, *46*, 339-342. In addition, F^- anion can abstract a proton from this solvent resulting in the slow formation of the bifluoride and acetonitrile anions. With chloroform or methylene chloride the F^- anion undergoes halogen exchange reactions at room temperature. Christe, K. O. Wilson, W. W. *J. Fluorine Chem.* **1990**, *47*, 117-120.
20. Pregosin P. S. in *NMR in Organometallic Chemistry*. Wiley-VCH, Chichester, 2012.
21. Conformations including the nitrogen atom of taniaphos in the coordination sphere of silver are energetically less stable (see Supporting Information).
22. Cabrera, S.; Gómez-Arrayás, R.; Martín-Matute, B.; Cossío, F. P.; Carretero, J. C. *Tetrahedron* **2007**, *63*, 6587-6602.

23. Note that *endo*-**7a** cycloadduct corresponds to (1*S*,3*R*,3a*S*,6a*R*)-**7a** whereas *ent*-*endo*-**7aa** corresponds to (1*R*,3*S*,3a*R*,6a*S*)-**7aa**.